

Original Article

Electrical stimulation induced pre-vascularization of engineered dental pulp tissue

Ying-tong Wang^{a, b}, Jia-ying Zhou^a, Kai Chen^c, Xiao Yu^a, Zhi-yong Dong^a, Yu-shan Liu^a, Xiao-ting Meng^{a, *}^a Department of Histology & Embryology, College of Basic Medical Sciences, Jilin University, Changchun, China^b The Undergraduate Center of Hospital of Stomatology, Jilin University, Changchun 130021, China^c Norman Bethune Stomatological School of Jilin University, Changchun 130021, China

ARTICLE INFO

Article history:

Received 8 April 2024

Received in revised form

16 June 2024

Accepted 20 June 2024

Keywords:

Electric field

Pre-vascularized dental pulp tissue

Dental pulp stem cells

Human umbilical vein endothelial cells

ABSTRACT

Vascularization is a key step to achieve pulp tissue regeneration and *in vitro* pre-vascularized dental pulp tissue could be applied as a graft substitute for dental pulp tissue repair. In this study, human dental pulp stem cells (DPSCs) and human umbilical vein endothelial cells (hUVECs) were co-cultured in 3D Matrigel and 150 mV/mm electric fields (EFs) were used to promote the construction of pre-vascularized dental pulp tissue. After optimizing co-cultured ratio of two cell types, immunofluorescence staining, and live/dead detection were used to investigate the effect of EFs on cell survival, differentiation and vessel formation in 3D engineered dental pulp tissue. RNA sequencing was used to investigate the potential molecular mechanisms by which EF regulates vessel formation in 3D engineered dental pulp tissue. Here we identified that EF-induced pre-vascularized engineered dental pulp tissue not only had odontoblasts, but also had a rich vascular network, and smooth muscle-like cells appeared around the blood vessels. The GO enrichment analysis showed that these genes were significantly enriched in regulation of angiogenesis, cell migration and motility. The most significant term of the KEGG pathway analysis were NOTCH signaling pathway and Calcium signaling pathway etc. The PPI network revealed that NOTCH1 and IL-6 were central hub genes. Our study indicated that EFs significantly promoted the maturation and stable of blood vessel in 3D engineered pulp tissue and provided an experimental basis for the application of EF in dental pulp angiogenesis and regeneration.

© 2024 The Author(s). Published by Elsevier BV on behalf of The Japanese Society for Regenerative Medicine. This is an open access article under the CC BY-NC-ND license (<http://creativecommons.org/licenses/by-nc-nd/4.0/>).

1. Introduction

Root canal therapy is currently the preferred treatment for irreversible pulpitis in mature permanent teeth, which mainly involves the removal of infected pulp tissue and the mechanical filling of inert materials such as gutta tips in the root canal to form a physical barrier [1]. However, due to the permanent inactivation of the tooth after root canal treatment, the lack of blood supply and nerve innervation of the tooth tissue often leads to unacceptable complications such as tooth fracture and tooth loss. It is widely accepted that the ideal pulp tissue regeneration should meet the following requirements: (1) abundant blood vessels in the tissue;

(2) the regenerated tissue included odontoblast layer and dentin; (3) functional pulpal nerves [2]. Among these, the rich capillary network in dental pulp is the structural basis for the nutritional function and regeneration of dental pulp. Therefore, the rapid formation of a functional vascular network is a decisive factor for pulp tissue regeneration. In recent years, many studies have proposed pre-vascular techniques to preform functional vascular networks in the engineered tissue structure of the dental pulp to ensure the rapid delivery of adequate blood supply [3] and eventually induce regeneration of the vascularized dental pulp [4]. Compared with traditional methods, this method can precisely control the formation of vascular networks *in vitro*, accelerate the vascularization process *in vivo*, and facilitate large-scale production and clinical translation [5].

The development of pre-vascular techniques in the field of dental pulp regeneration originated from attempts to construct blood vessels with endothelial cells (ECs) [6]. ECs line the inner

* Corresponding author.

E-mail address: mengxt@jlu.edu.cn (X.-t. Meng).

Peer review under responsibility of the Japanese Society for Regenerative Medicine.

surface of blood vessels and form the inner wall, which is an integral part of the process of blood vessel formation. ECs, such as human umbilical vein endothelial cells (hUVECs), human umbilical artery endothelial cells, human microvascular endothelial cells, and endothelial progenitor cells, are the most direct cell sources that minimizes the risk of immune rejection.

On the other hand, human teeth have a unique structure in which the internal pulp is enclosed by a thick dentin wall and the pulp tissue is connected to the surrounding tissue. Dental pulp stem cell (DPSC) is a type of mesenchymal stem cell (MSC) with great potential for dental pulp repair and regeneration and is ideal seed cell for the construction of dental pulp tissue *in vitro*. Furthermore, in dental pulp tissue, DPSCs are the main microenvironmental factors affecting angiogenesis. Studies have shown that DPSCs promote early vascular network formation by promoting the migration of HUVECs and increasing the expression of vascular endothelial growth factor (VEGF) [7].

Although several studies have demonstrated successful formation of microvascular networks in engineered pulp tissues, rapid formation of a stable mature vascular network which is highly organized, branched and dense is still far away from clinical application [1].

Recent studies have shown that electrical stimulation (ES) is expected to promote angiogenesis. It has been documented that endogenous electric fields (EFs) generated by blood flow affect arterial diameter by increasing endothelial secretion of NO. In addition, capillary density increased by 25% after 6 weeks of treatment with ES [8]. Experiments have shown that ES not only affects the directional migration, proliferation and elongation of ECs, but also increases the length of tubular structures and promotes the expression of vascular endothelial growth factor (VEGF). VEGF expression thereby increased the rate of blood vessel formation [9,10]. Most importantly, ES also promotes the differentiation and angiogenesis of MSCs, which may further promote the vascularization of engineered tissue [11,12].

In this study, DPSCs and hUVECs were co-cultured in 3D Matrigel and 150 mV/mm electric fields were used to promote the construction of pre-vascularized dental pulp tissue. After optimizing co-cultured ratio of two cell types, immunofluorescence staining and live/dead detection were used to investigate the effect of EFs on cell survival, differentiation and vessel formation in 3D engineered dental pulp tissue. RNA sequencing was used to investigate the potential molecular mechanisms by which EF regulates vessel formation in 3D engineered dental pulp tissue. The aim of this study is to provide an experimental basis for the application of ES in dental pulp angiogenesis and regeneration.

2. Methods

2.1. Isolation and expansion of DPSCs

Intact third molars from patients aged 18–22 years were obtained and immersed in 0.01M PBS containing 20% penicillin and streptomycin and stored in an ice box. After the teeth were split, the

fresh pulp was taken out and put into a small dish. The pulp tissue was minutely chopped with a double blade method. Then the pulp tissue was transferred into a 15 mL centrifuge tube, and an appropriate volume of collagenase type I (3 mg/mL, Solarbio, C8140) and Dispase II (4 mg/mL, Solarbio, D6431) were added. The mixture was mixed and digested thoroughly for 60 min. Digestion was terminated by adding α -MEM medium (GIBCO, 12571063) containing 10% fetal bovine serum (FBS, Hyclone, SH30406), centrifuged at 1000 rpm for 5 min, and the supernatant was discarded. Finally, the fragment of pulp tissue was resuspended in the MSC medium (MSCM, DAKWE, b114011) containing 10% fetal bovine serum, and then mechanically separated into single cell suspensions or cell clusters. Cells were resuspended in MSC Medium and incubated at 37 °C in 5% CO₂ incubator. Changing the medium every 3 days until the cells reached 80% confluence for subculture. DPSCs isolated from five human donors were characterized and used individually in triplicate experiments.

HUVECs (gift obtained from Dr. Wang) were cultured in endothelial cell medium (10% FBS 1640, Gibco, C11875500BT) at 37 °C with 5% CO₂. Cells from passages 3 to 6 of each cell type were used in all experiments.

2.2. Identification of DPSCs surface markers by flow cytometry

To identify the MSC characteristics of DPSCs, about 1×10^6 /mL DPSCs per EP tube were collected and assessed by flow cytometric analysis (BD FACS Calibur flow cytometer). The working concentrations of primary antibodies were summarized in Table 1.

2.3. Multilineage differentiation of DPSCs

To induce adipogenic and osteogenic differentiation, 1×10^5 DPSCs per well were seeded in pre-gelatin-coated 24-well plates and then incubated in adipogenic (DAKEWE, 6114531) and osteogenic differentiation-inducing media (DAKEWE, 6114541) respectively for 21 days with regular media changes. After 21 days of induction in differentiation-inducing media, the cells were fixed with 4% paraformaldehyde and then stained with oil red O (DAKEWE, 4060711) or alizarin red (DAKEWE, 4060611) respectively. Followed by using an inverted microscope to photograph.

2.4. Histology and immunochemical staining

For immunochemical staining, the cells were washed 3 times with PBS then fixed with 4% paraformaldehyde for 20 min at room temperature. After washing with PBS thrice, 10 min of 0.03% TritonX-100 and 20 min 5% BSA treatment were carried out in sequence. All samples were incubated in appropriate proportion of primary antibodies (Table 2) respectively at 4 °C overnight. Washing 4 times with PBS, secondary antibody (1:100; Life Technology, A11010, A11008 and A21143) was then added and incubated for 60 min at room temperature. All samples were counter stained with DAPI for 10 min before imaging.

Table 1
List of antibodies for FACS.

Antibody	Species	Manufacturers/Cat.no.	Homologous control	Concentration
CD105	Mouse	eBioscience, 2270778	IgG1-PE	1:100
CD90	Mouse	eBioscience, 2279704	IgG1-FITC	1:200
CD73	Mouse	eBioscience, 2251944	IgG1-FITC	1:50
CD19	Mouse	eBioscience, 2285417	IgG1-FITC	1:2000
CD11b	Mouse	eBioscience, 2338659	IgG1-FITC	1:200
HLA-DR	Mouse	eBioscience, 2213079	IgG1-FITC	1:5000
IgG1-PE	Mouse	eBioscience, 2252682	IgG2b-FITC	1:300
IgG1-FITC	Mouse	eBioscience, 2273262	–	1:200
IgG2b-FITC	Mouse	eBioscience, 2204963	–	1:200

2.5. Optimization of DPSCs/HUVECs co-culture conditions

To analyze the effect of different co-culture ratios of DPSCs and HUVECs on cell tube formation, DPSCs and HUVECs were plated into the 50 μ l 3D Matrigel matrix in different ratios (DPSCs: HUVECs, 1:0; 5:1; 3:1; 1:1; 1:3; 1:5; 0:1) and supplemented with corresponding proportions of two different kinds of cell medium.

To quantify cell tube formation, co-cultured DPSCs/HUVECs at different cell proportions were placed in 96-well plates, each with three replicates, and cultured for 2–12 h. Microscopic images were taken every 2 h at 20 \times magnification in five random areas of each sample. ImageJ software (Angiogenesis Analyzer, National Institutes of Health, <https://imagej.nih.gov/ij/>) was used to analyze and measure the relative tube length, branch number and relative junction area of different groups.

The tube-like structure surrounded by CD31 positive cells was used for further evaluation of cell tube formation ability. The values are given as mean \pm standard deviation.

2.6. Live/dead staining

A fluorescent live/dead assay kit (calcein-AM/propidium iodide, Invitrogen, L32250) was used to assess the viability of encapsulated cells. Samples were incubated for 10 min with calcein-AM (1 mM) and propidium iodide (1 mg/mL). The samples were rinsed three times with PBS and then analyzed using a fluorescence microscope (IX 71, Olympus, Japan). The images were processed using ImageJ to remove background noise, and the cell count plugin was used to identify green and red fluorescent cell bodies. Green-fluorescent cells were considered as alive cells, and red-fluorescent cells were considered as dead cells. Cell viability was calculated as the percentage of living cells relative to the total number of cells.

2.7. Construction of engineered human dental pulp tissue in 3D Matrigel

DPSCs (P3–P5) and HUVEC cells in logarithmic growth phase were selected. After centrifugation, the culture medium was added and mixed with a pipette. The cell suspension was thoroughly mixed with 50 μ l pre-cooled Matrigel at a ratio of 1:5 in an ice bath (The Matrigel should be placed at 4 $^{\circ}$ C one day in advance). The Matrigel and the cell mixture were positioned in the middle of the culture dish as droplets. The plates were then placed in an incubator at 37 $^{\circ}$ C with 5% CO₂ for 15–30 min to allow Matrigel gelatinization. Subsequently, culture medium was added to the dish and the incubation was continued. The culture medium was changed every three days.

2.8. Electrical stimulation to induce angiogenesis in engineered human dental pulp tissue

Electrotactic chambers and electrical stimulation protocol were established as described previously with minor modifications [13]. Briefly, DPSCs and HUVECs were mixed well in 50 μ l Matrigel at an

optimized ratio on ice, and then the mixture was incubated at 37 $^{\circ}$ C to allow gelatinization. The next day, a cover slip was placed over the culture area, grease sealed both sides of the culture area so that the culture fluid could only flow through the 3D culture. Direct current (DC) EFs were applied to the 3D culture in an electrotactic chamber via 5% FBS agar bridges, and the cultures were treated with a physiological strength 150 mV/mm DC EFs in the medium. The co-cultured cells in 3D Matrigel were exposed to EFs for 30 min per day. Cultures were analyzed at different timepoints by immunocytochemical staining following by confocal imaging.

2.9. RNA extraction and sequencing analysis

Total RNA was extracted on site by the company (Biomarker, China) performing sequencing. Sequencing and preparation of Illumina libraries was performed and then sequenced Illumina libraries were generated using the Hieff NGS Ultima Dual-mode mRNA Library Prep Kit (Yeasen Biotechnology (Shanghai) Co., Ltd., 12309ES08). An index was added to the sequence of each sample. Libraries were sequenced on an Illumina NovaSeq platform to generate 150-bp double-terminal sequences. Raw readings were further processed using the bioinformatics analysis platform BMK Cloud (www.biocloud.net). Raw data in Fastq format is first processed by in-house perl scripts. The Hisat2 tool software was used to align the valid data to the reference genome sequence. Differential expression analysis was performed by comparing the EF and NO EF control groups. *P*-values were adjusted by the Benjamini & Hochberg method using the DESeq2 R software package. An adjusted *P* value of 0.05 and a Fold Change of 1.5 were used as the threshold for significant differential expression. For enrichment analysis of differentially expressed genes, GO and KEGG enrichment analyses were performed by using cluster analysis R package, and gene length bias was corrected. A corrected *p*-value of less than 0.05 was considered to be significantly enriched for differentially expressed genes. The cluster profile package was used to select the pathways related to angiogenesis for display. To explore potential interaction relationships between DEGs, protein–protein interaction (PPI) analysis was also performed based on the STRING database (<https://string-db.org/cgi/input.pl>). Cytoscape 3.8.2 software was used to visualize the PPI network. The RNA-seq data in this study was submitted to Gene Expression Omnibus (GEO) (<http://www.ncbi.nlm.nih.gov/geo/>) under accession ID GSE174619.

2.10. RT-qPCR analysis

Total RNA was isolated from MSC and differentiated cells using TRIzol[®] reagent (Invitrogen, 1596026CN) after osteogenic and adipogenic induction. 0.5 mg of purified total RNA was reverse transcribed into cDNA using HiScript III 1st Strand cDNA Synthesis Kit (+gDNA wiper) (Vazyme, R323) following the manufacturer's protocols. qPCR reactions were performed using ChamQ Universal SYBR qPCR Master Mix (Vazyme, Q711) in Light Cycle 480 II Real-Time PCR Detection System (Roche) with the conditions presented in Table 3. GAPDH was used as a reference gene. The primer sequences of RUNX2, ALPL, ADIPOQ, PPARG2 and GAPDH are presented in Table 3. The relative expression of target genes was determined using the 2^{- $\Delta\Delta$ Cq} method and normalized to GAPDH. All the reactions were performed in triplicate.

2.11. Statistical analysis

All data were analyzed by t-test and one-way ANOVA test to determine statistical significance and were expressed as mean \pm standard deviation. *P* < 0.05 was considered as significant difference.

Table 2
List of antibodies for Immunofluorescent chemical staining.

Antibody	Species	Manufacturers/Cat.no.	Concentration
CD90	Mouse	Abcam, ab307736	1:200
CD34	Mouse	Abcam, ab81289	1:100
CD31	Rabbit	Zenbio, 347526	1:200
DSPP	Rabbit	Bioss, bs-10316R	1:200
α SMA	Mouse	Bioss, bsm-33187M	1:700
Nestin	Mouse	Arigobio, ARG52345	1:400
Reelin	Rabbit	Bioss, bs-1560R	1:200

Table 3
Primers used for reverse transcription-quantitative PCR.

Gene	Primer sequences (5' → 3')	Size (bp)	Amplified conditions
RUNX2	F:AGGCAGTTCCCAAGCATTTTCATC R:AGTGAAGTGGTGGCGGACATAC	133	Stage1 : 95 °C 30 s (1×)Stage2 : 95 °C 10s 60 °C 30 s (40×)
ALPL	F:CACCGCCACCGCTACC R:CACAGATTTCCAGCGTCCITG	148	Stage3 : 95 °C 15s 60 °C 60s
ADIPOQ	F:GCATTCAGTGTGGGATTGGAGAC R:ATTTACCAGTGGAGCCATCATAGTG	109	95 °C 15 s (1×)
PPARG2	F:TGAATCCAGAGTCCGCTGACC R:CGCCTCGCCTTTGCTTTG	95	

RUNX2 (Runt-related transcription factor 2); ALPL (Alkaline Phosphatase, Liver/Bone/Kidney); ADIPOQ (Adiponectin); PPARG2 (Peroxisome proliferator activated receptor gamma); F, forward; R, reverse.

3. Results

3.1. Human DPSCs were isolated from human dental pulp tissue

The pulp tissues were separated from the roots of the teeth (Fig. 1A), after 96 h of culture, many of the cells migrated out from the fragment of pulp tissues (Fig. 1B). The DPSCs showed typical morphological characteristics of MSCs when cultured in 2D, the cells were spindle-shaped and elongated, arranged in parallel with each other (Fig. 1C). As shown in Fig. 1D, the CD73, CD90 and CD105 positive cells were 97.78%, 99.85% and 99.24% respectively. On the contrary, the CD19 and CD11b positive cells were only 0.77% or 0.67% respectively. Immunofluorescence chemical staining further confirmed that the DPSCs were CD90 positive and CD34 negative cells (Fig. 1E and F). These results identified that the isolated DPSCs were positive for mesenchymal markers CD73, CD90 and CD105 while negative for hematopoietic markers the CD19, CD11b and CD34.

Furthermore, we investigated the ability of DPSCs to differentiate into two lineages. After 21 days of osteogenic induction, the cells grew in clusters, formed clonal-like protrusions, and showed large reticular rough surface processes. After alizarin red S staining, the clonal-like bulge showed typical orange-red calcium deposits with specific pigmentation (Fig. 1G). When DPSCs were differentiated in adipogenic induction media, small transparent lipid droplets gradually appeared in the cells, and the cell volume gradually increased. Oil Red O-stained lipid droplets were clearly visible in the cells, indicating adipogenic differentiation (Fig. 1H). RT-qPCR results further showed that the osteogenic specific genes RUNX2 (Runt-related transcription factor 2) and ALPL (Alkaline Phosphatase, Liver/Bone/Kidney), adipogenic specific genes ADIPOQ (Adiponectin) and PPARG2 (Peroxisome proliferator activated receptor gamma) were significantly up-regulated during osteogenic and adipogenic differentiation, respectively (Fig. 1I).

3.2. Different co-culture ratios of DPSCs/HUVECs affect endothelial cell tube formation in 3D Matrigel matrix

Although it has been shown that 1:1 ratio co-culture of DPSCs with HUVECs promotes angiogenesis through VEGF secretion. The cellular growth behavior and cell physiological status in the 3D microenvironment are quite different from that in the 2D microenvironment. Therefore, it is necessary to further investigate the co-culture ratios of DPSCs/HUVECs to construct the vasculature-rich 3D dental pulp tissue. DPSCs and HUVECs were seeded into the 3D Matrigel matrix in different proportions (Fig. 2A). After 4–6 h of co-culture, the clear tubular structure could be observed under the microscope. HUVECs were gradually arranged to form

capillary-like structures, and the interconnected capillaries formed a network structure in the 3D Matrigel (Fig. 2A). After 8 h of culture, the ImageJ plugin Angiogenesis Analyzer was used to assess various indicators of the tubular structures formed by HUVEC cells. The results are shown in Fig. 2B, C, D and E. These results indicated that the number of junctions, branches, the mean mesh size, and total branching length are reached 270.83 ± 45.58 , 212.53 ± 9.11 , 16195.6 ± 2504.25 and 27788.8 ± 2895.91 respectively in the co-culture ratio of 1:3, significantly more than those of other co-culture groups.

3.3. Electrical stimulation promoted the vascularization of co-cultured cells in 3D matrix

3.3.1. Electrical stimulation didn't affect cell survival in 3D matrix

It has been well documented that 150 mV/mm EFs are sufficient to induce the migration, orientation and elongation of epithelial cell, thus promoting vasculogenesis [14–16]. Here we seeded DPSCs and HUVECs into 3D Matrigel matrix at a ratio of 1:3 and stimulated with 150mv/mm DC current for 30 min per day. Live/Dead assay showed that there was no significant difference in cell death rate between EF group and NO EF group. This indicated that the EF intensity of 150 mV/mm had no significant effect on the viability of the co-cultured cells in 3D matrix (Fig. 3A and B).

3.3.2. Electrical stimulation promoted the formation of vessel

When co-cultured DPSCs/HUVECs were stimulated by 150 mV/mm EFs, vascular tubes were formed and increased with time. The investigation of the formation of endothelial tubules and blood vessel network were carried out at day1, day2 and day3 of culture respectively. Interestingly, comparing the vessel maturation in EF group to it in NO EF group, development revealed more complex engineered vessel-like structures and blood vessel networks with EF-stimulation, emphasizing the importance of EF-stimulation in tube formation (Fig. 3C).

ImageJ plugin Angiogenesis Analyzer was used to measure the relative tubular length of the different groups. Compared with the group without EF-stimulation, EFs significantly increased the number of junctions, branches, the mean mesh size, and total branching length in 3D Matrigel, which were twofold more in EF group compared with NO EF group (Fig. 3D, E, F and G). It is worth to note that the number of junctions, branches and the mean mesh size reached 296 ± 96.82 , 241 ± 32.95 and 3275.91 ± 476.02 respectively on the second day of EF-stimulation, while the No EF stimulation group had these numbers or even less (215.3 ± 82.53 , 195 ± 71.47 and 2741.1 ± 836.44 respectively) on the third day. By day 3, flourishing vessel networks were observed throughout the construct, with fourfold more junction points compared with day 1

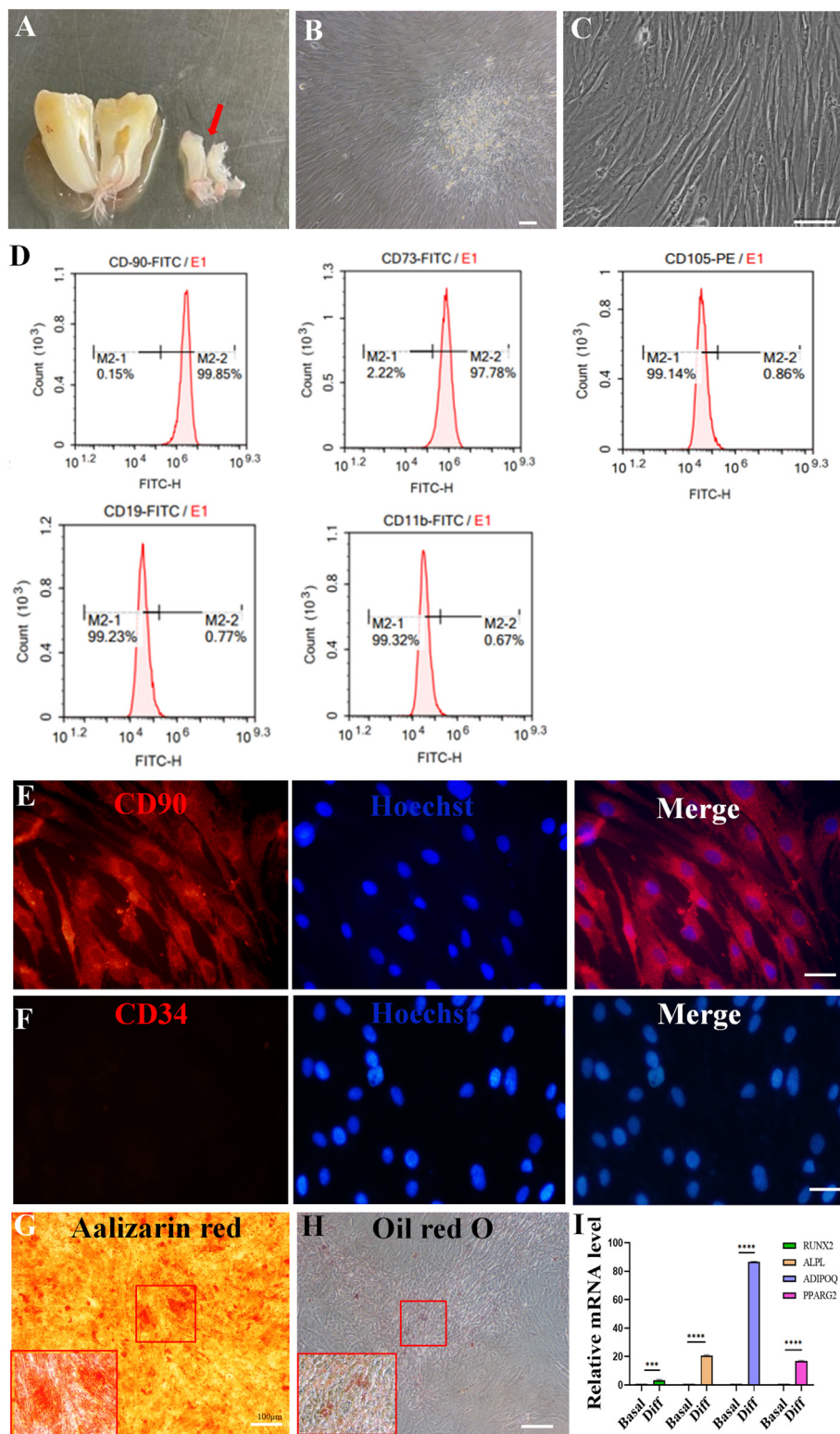


Fig. 1. Identification of mesenchymal stem cell properties of DPSCs. A: The pulp tissues were separated from the roots of the teeth. B and C: The DPSCs showed typical morphological characteristics of MSCs. D: Specific marker analysis of DPSCs by flow cytometry. E: Anti-CD90 immunofluorescence chemical staining. F: Anti-CD34 immunofluorescence chemical staining. G: Alizarin red staining after osteogenic differentiation of human DPSCs for 21 days. H: Oil red O staining after adipogenic differentiation of human DPSCs for 21 days. I: Reverse transcription-quantitative PCR analysis of RUNX2, ALPL, ADIPOQ and PPARG2 gene expression in MSCs after 21 days of culture in osteogenic or adipogenic versus basal conditions. n = 3 (***P < 0.001; ****P < 0.0001). Scale bars represent 50 μ m.

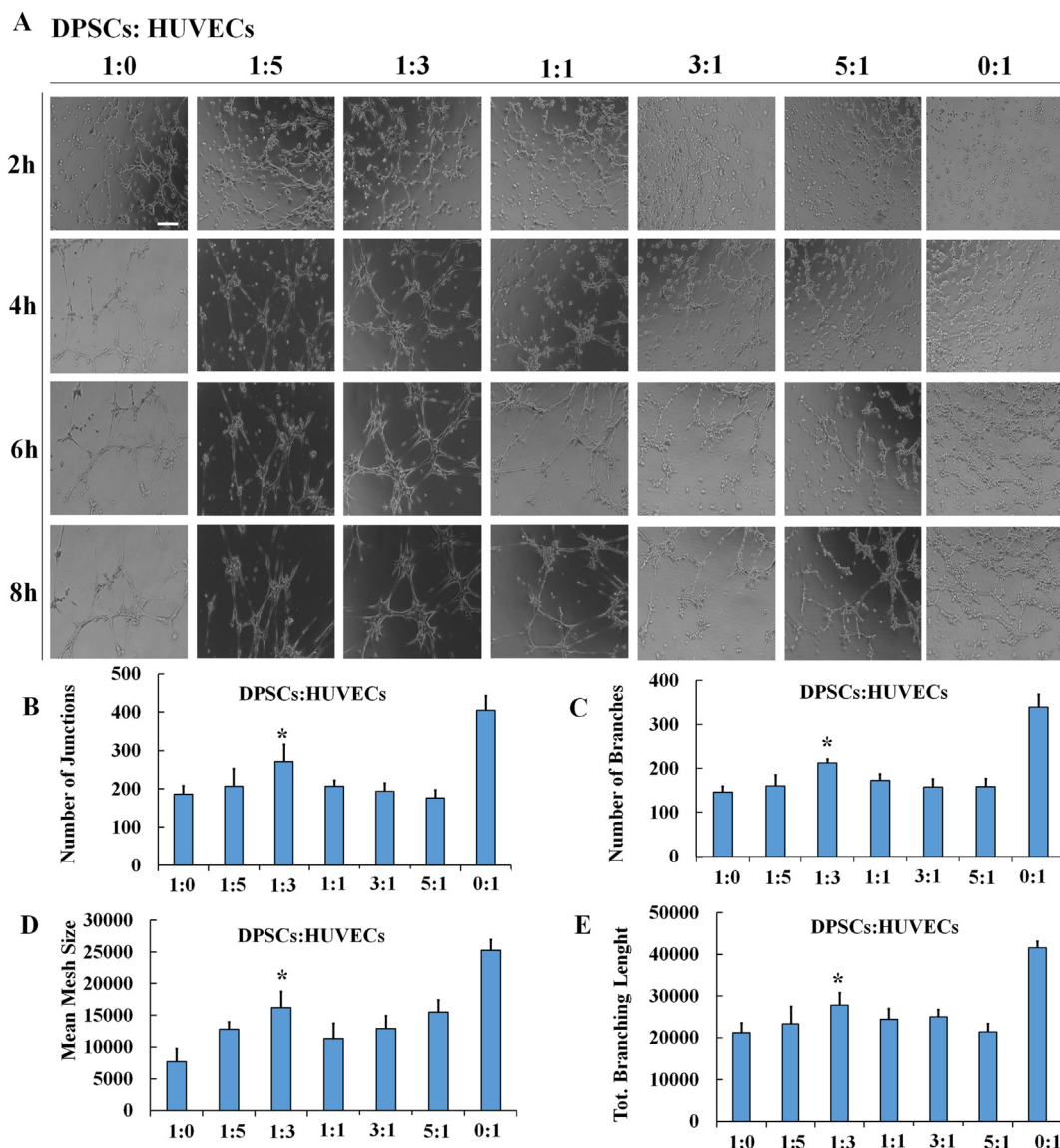


Fig. 2. The effect of co-culture ratios of DPSCs and HUVECs on tube formation in 3D Matrigel. A: Tube-like structures formed by different proportions of cells co-cultured in 3D Matrigel. Average of the number of junctions (B), branches (C), the mean mesh size (D), and total branching length (E) were analyzed by the ImageJ plugin Angiogenesis Analyzer. Data are presented as means ± SEM. n ≥ 3 (*P < 0.05). Scale bar represents 100 μm.

in EF group, indicating that EFs accelerated vessel formation and maturation in 3D Matrigel.

3.4. Co-cultured DPSCs differentiated into odontoblasts, pericytes or smooth muscle cells in 3D vascularized tissue

To examine the cellular composition in the vascularized dental pulp tissues induced by electrical stimulation, immunofluorescence staining was used to identify the expression of specific biological markers, including dentin phosphoprotein (DSPP), Nestin, Reelin and α-SMA. DSPP and Nestin are specific markers of odontoblasts. Reelin is always expressed in secretory odontoblasts. α-SMA is expressed in vascular pericytes, myofibroblasts and smooth muscle cells. The con-focal images showed that both DSPP and α-SMA were positively expressed in engineered pulp tissue on day 7 of culture but the two proteins did not colocalize (Fig. 4A and B). We noticed that the distribution of α-SMA positive cells were observed along the vessel border, which explains the presences of vascular pericytes, myofibroblasts or smooth muscle cells in the engineered

dental tissue. In contrast, Nestin and Reelin expression showed colocalization in the cells (Fig. 4C). The expression of Nestin or Reelin was serrated and found in ring-shaped structures.

3.5. Gene ontology functional analysis and the enrichment of KEGG signaling pathway for EF-regulated vascularization in 3D engineered dental pulp tissue

To assess the overall gene changes following vascularization in 3D engineered dental pulp tissue, 6 samples were carried out with EF or NO EF respectively for 7 days and RNA sequencing was performed as described in the methods. After the alignment of RNA-Seq data to the human genome hg38. A total of 12661 genes were obtained from the intersection set of control and experimental results (Fig. 5A). Of these, 189 genes had significant expression difference, including 64 up-regulated genes and 125 down-regulated genes (Fig. 5B).

ClusterProfiler software performed GO functional enrichment analysis (Fig. 5C) and KEGG pathway enrichment analysis of the

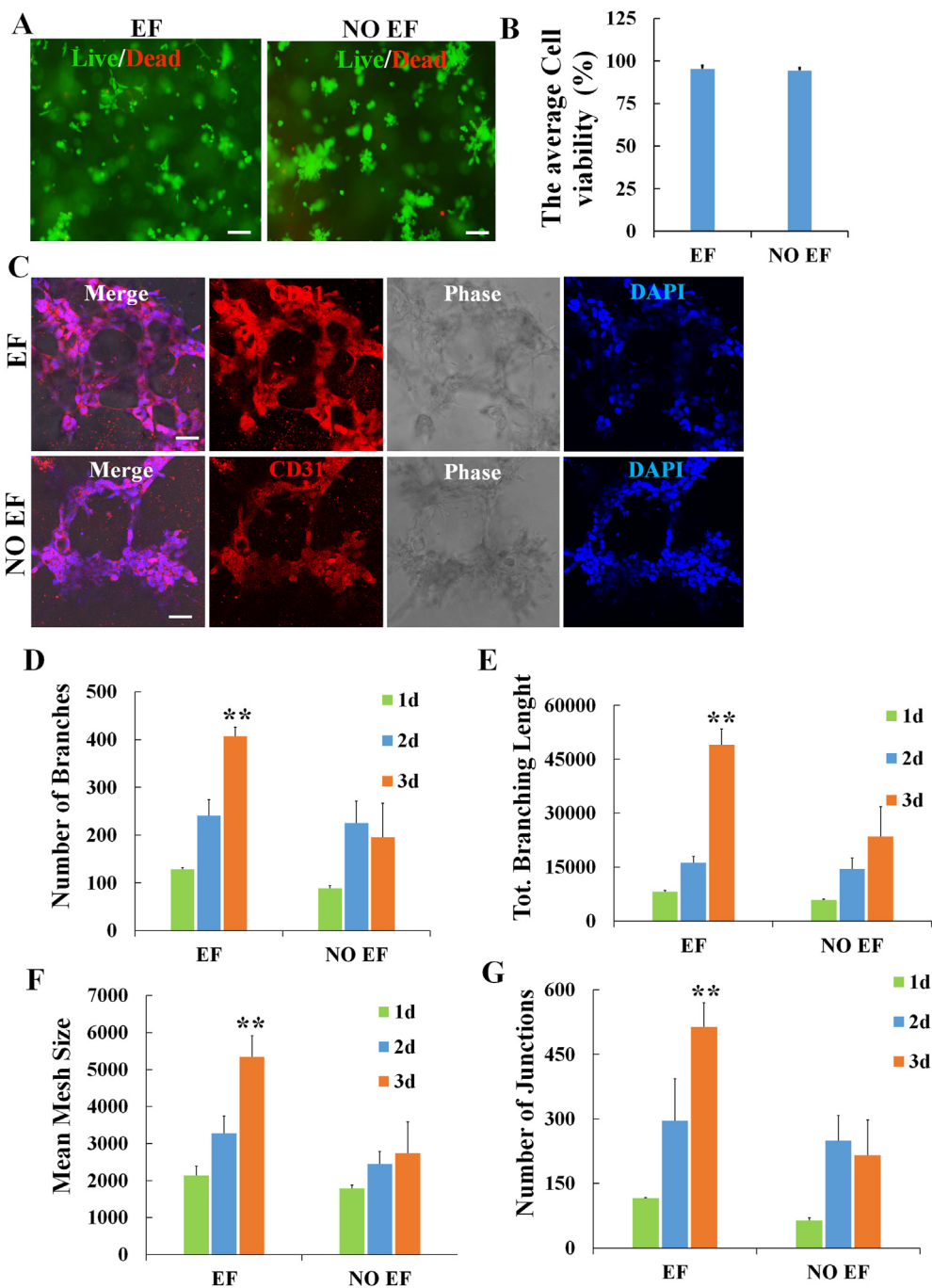


Fig. 3. Electrical stimulation promoted the vascularization of co-cultured cells. A: live/dead staining cells were observed by fluorescence microscope (green fluorescence showed live cells, red fluorescence showed dead cells). B: statistical analysis of the average cell viability in EF group and NO EF group. C: Anti-CD31 immunofluorescence staining showed tubular structures surrounded by CD31-positive cells in EF group and NO EF group. D–G: statistical analysis of number of branches, branches length, mean mesh size and number of junctions at different time points of culture. Data are presented as means ± SEM. Student T-test and one-way ANOVA, $n \geq 3$ (** $p < 0.01$). Scale bars represent 100 μ m.

differential gene set (Fig. 6). For results of GO functional enrichment, a p -value < 0.05 was used as the threshold for significant enrichment. The DEGs were classified into three functional groups, including biological process, cellular component and molecular function. The top 30 enriched GO biological processes of all DEGs. The results mainly involved regulation of angiogenesis, response to wounding, cellular component movement, cell migration and cell motility.

KEGG pathway enrichment mainly included the following pathways: NOTCH signaling pathway, Calcium, IL-17, Hedgehog,

Estrogen, TNF, MAPK and PI3K-AKT signaling pathway etc (Fig. 6A and B). Most notable pro-angiogenic genes that shown increased expression were NOTCH1, HES1, NBP26, NGFR, MEF2C etc.

3.6. PPI networks of the DEGs in EF group and NO EF group

It is well known that vascular growth in particular tissue involves a specialized, tissue-specific form of angiogenesis [17], and PPI network could help us to further extract the hub genes in the

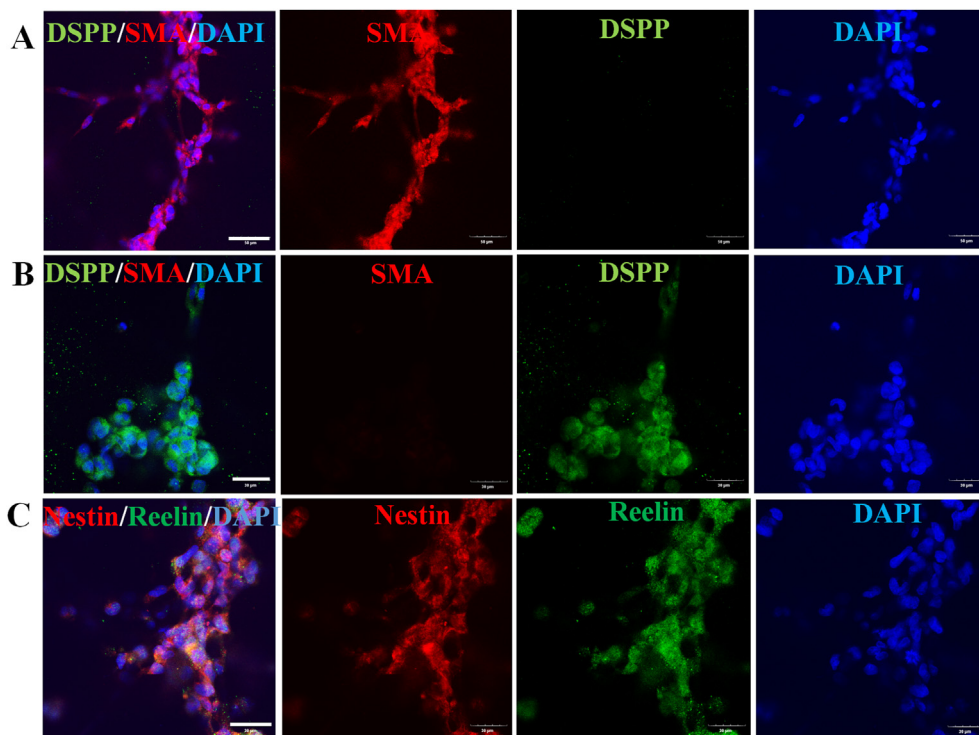


Fig. 4. Immunofluorescence observations of DSPP, α -SMA, Nestin and Reelin in the dental pulp-like 3D engineered tissue at Day 7 after EF-stimulation. Representative fluorescent images of DPSC/HUVEC 3D cocultures probed for α -SMA (red)/DSPP (green) (A and B) and Nestin (red)/Reelin (green) (C), and nuclei (DAPI, blue), A: scale bar represents 50 μ m; B and C: scale bars represent 30 μ m.

process of ES-regulated angiogenesis in 3D Matrigel. In this research, PPI network of the DEGs related to the regulation of angiogenesis was constructed (adjusted $P < 0.05$) by the KEGG pathway analysis in EF group and NO EF group. In the PPI networks of 86 DEGs, there were 86 nodes and 264 edges. Among them, 7 genes were extracted: NOTCH1, SNAIL, IL-6, DNER, FOS, SPHK1, and KCNQ4. NOTCH1 and IL-6 were central hub genes in the network, with the number of degree ($n = 14$) (Fig. 7).

4. Discussion

The aim of our study was to define a more efficient and clinically relevant method for the construction of pre-vascularized human dental pulp tissue. Although there have been reports that when co-cultured with HUVEC, DPSC plays a role in angiogenesis by enhancing HUVEC migration and VEGF secretion [18]. However, engineered dental pulp tissue vascularization always faces the difficult problems such as slow speed of vascular network establishment and poor vascular stability [19].

In this study, the co-cultured DPSCs and HUVECs were used to construct the pre-vascularized engineered dental pulp tissue. The engineered dental pulp tissue not only had odontoblasts, but also had a rich vascular network, and smooth muscle-like cells appeared around the blood vessels. And ES significantly increased the number of connections and total branch length of endothelial network in the 3D engineered pulp tissue and resulted in improved angiogenesis.

Pre-vascularized dental pulp tissue requires the co-culture of DPSCs and HUVECs to form dentin cells and vascular networks. Therefore, we first screened the co-culture ratio of DPSCs and HUVECs, and then implanted the cells into 3D Matrigel at the optimal co-culture ratio of 1:3. The ES intensity of 150 mV/mm, which has been widely proved to be effective to induce tube

formation of HUVECs in 2D environment and this intensity did not cause significant cell death. However, the experimental evidence in 3D environment needs further evaluation, such as cell composition, vascular maturation of dental pulp tissue and the regulated mechanism.

The results of immunofluorescence analysis showed that the pre-vascularized dental pulp tissues contained dentin cells/odontoblasts, endothelial cells and pericytes or smooth muscle cells. We detected the DSPP, Nestin, Reelin and α -SMA positive cell in the 3D pre-vascularized dental pulp tissues. Differentiated odontoblasts could not be identified by one unique phenotypic marker, but the combination of expression of DSPP or Nestin may be valuable for the assessment of these cells. On the other hand, Reelin is always expressed in secretory odontoblasts and may be a key molecule in the relationship between odontoblasts and nerve fibers [20,21]. α -SMA is a cytoskeletal protein that is also localized in some stem cells and precursor cells and is considered to be one of the stem cell markers in dental pulp. α -SMA is also expressed in vascular pericytes, myofibroblasts and smooth muscle cells, and plays a key role in wound healing and participates in dental pulp healing [22]. During dentin formation, the majority of MSCs were identified to be located in the perivascular area, which is considered as a stem cell niche [23], and in this study, α -SMA positive cells were observed in the perivascular area.

Previous studies have demonstrated that endothelial cells will self-assemble into vascular networks within hydrogel, but these networks often regress within a few days in the absence of mural cells such as fibroblasts, smooth muscle cells, or pericytes. In this study, we still observed stable vascular-like structures after 7 days of electrical stimulation, which may be closely related to the formation of α -SMA positive cells around the tube.

How bioelectrical signals are transformed into intracellular signaling systems that initiate a range of cellular responses has

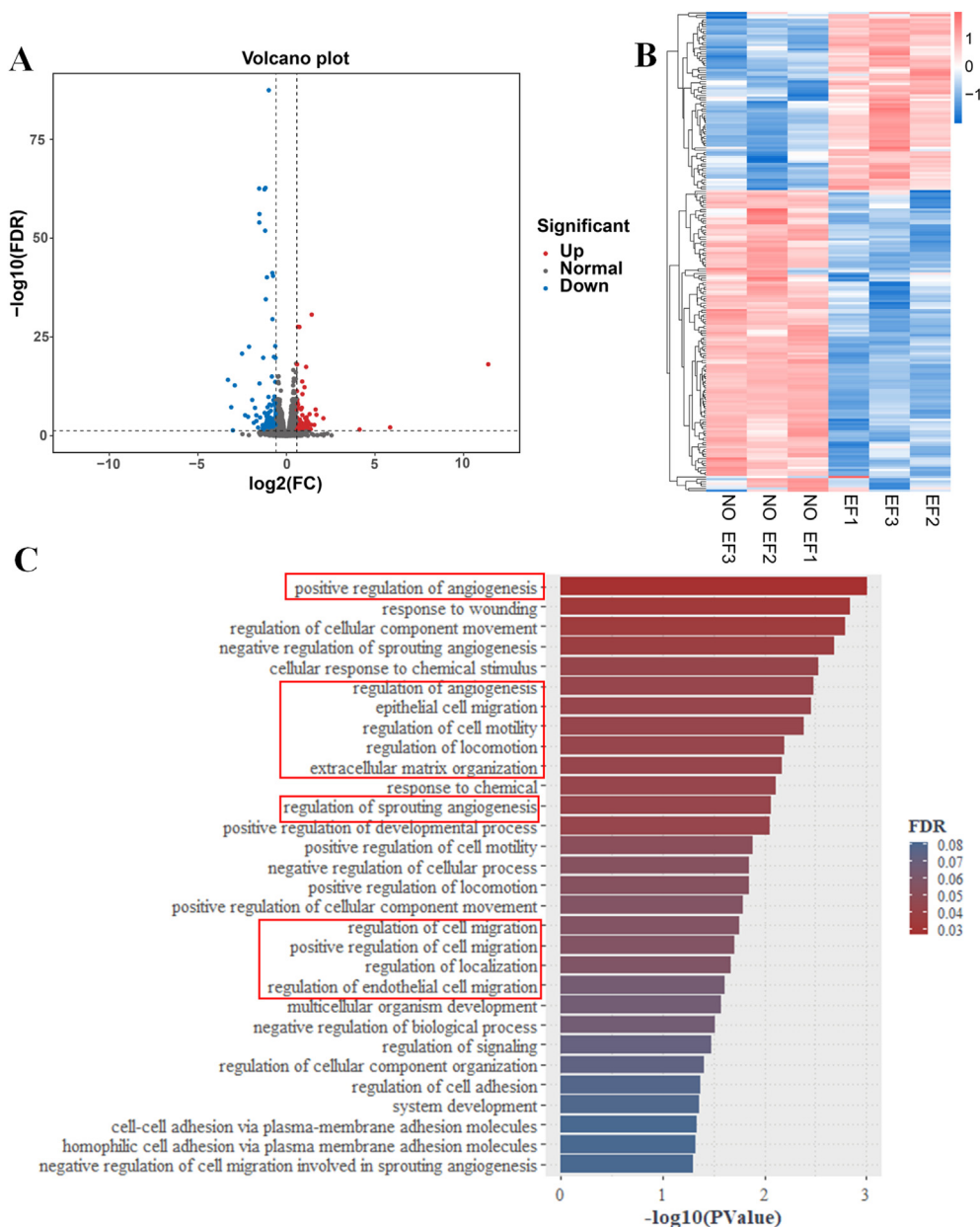


Fig. 5. GO functional enrichment analysis. A: The volcano plot showing the expression pattern of DEGs in EF and control group. B: Hierarchical clustering analysis of the DEGs in EF group and NO EF group. Red and blue bar charts represent significantly upregulated and downregulated genes, respectively. C: GO annotation was performed using 189 DEGs in EF and NO EF group to obtain insights into their biological functions.

been studied in a variety of cell types. It is generally accepted that bioelectrical signals can activate ion channels and that some voltage-sensitive genes or receptors on the cell membrane initiate downstream signaling pathways, resulting in various biological responses [24]. For instance, EFs mediated the directional migration of neural stem cells through the activation of a voltage-sensitive gene Phosphatidylinositol 3-kinase (PI3K) [25]. Notably, the genes and signaling pathways activated by ES were diverse across different cell types and microenvironments.

Here, RNA-Seq was used to analyze global gene expression for HUVECs during EF-induced vascular network formation in 3D engineered dental pulp tissue. The DEGs were classified into three functional groups, including biological process, cellular component and molecular function. The results mainly involved

regulation of angiogenesis, cellular component movement, cell migration and cell motility. KEGG pathway enrichment mainly included the following pathways: NOTCH signaling pathway, Calcium, IL-17, Hedgehog, Estrogen, TNF, MAPK and PI3K-AKT signaling pathway etc. It is well known that vascular growth in particular tissue involves a specialized, tissue-specific form of angiogenesis [17], and PPI network could help us to further extract the hub genes in the process of ES-regulated angiogenesis in 3D Matrigel. Here, 7 genes were extracted: NOTCH1, SNAIL, IL-6, DNER, FOS, SPHK1, and KCNQ4. NOTCH1 and IL-6 were central hub genes in the network.

It has been reported that NOTCH signaling system is one of the major pathways mediating angiogenesis through receptors for vascular endothelial growth factor (VEGF) [26], participating in tip-

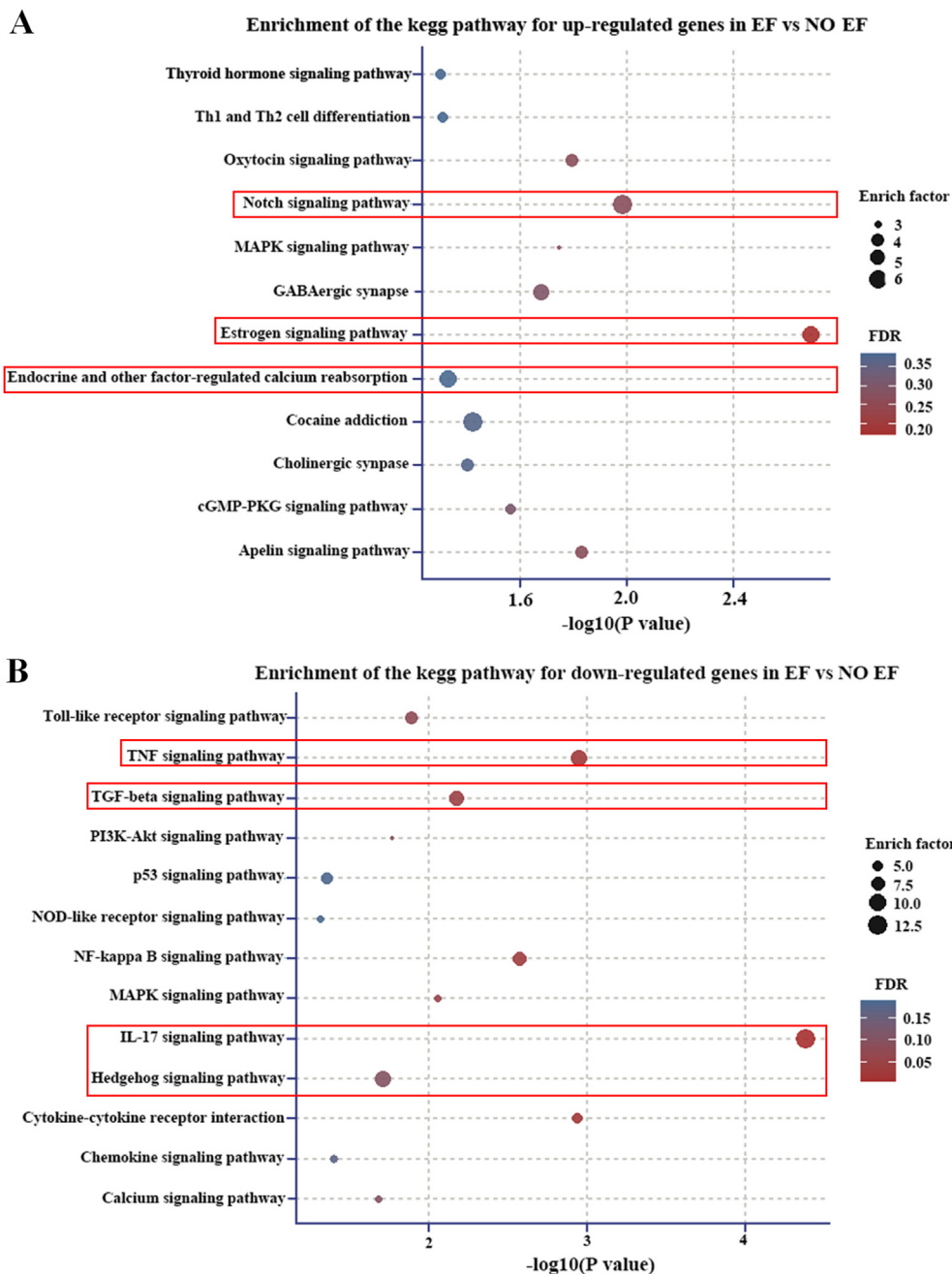


Fig. 6. The KEGG signaling pathway enriched by the DEGs. KEGG annotation was performed using DEGs in EF and NO EF group to obtain insights into their pathways involved. A: The top 12 enriched KEGG pathways of the upregulated DEGs. B: The top 12 enriched KEGG pathways of the downregulated DEGs.

stalk specification, arterial-venous differentiation, vessel stabilization, and maturation processes [27]. It is essential for the development of tip and stalk EC via Notch signalling. Ramasamy et al. reported that Notch signaling promotes EC proliferation and vessel growth in postnatal long bone, which is the opposite of the well-established function of Notch and its ligand Dll4 in the endothelium of other organs and tumors [17].

Snail is key factors of TGF-β and Notch signaling pathways to promote migration, proliferation and angiogenesis of

differentiated-endothelial cells [28,29]. And Notch receptors have been shown to regulate Snail family of proteins in specific types of endothelial cells [30,31].

It is interesting that inflammatory factor and NOTCH signaling pathways are essential for regulating the pro-angiogenic factors. Inflammatory cytokine interleukin-6 (IL-6) siRNA significantly reduced the expression of VEGF, VEGF receptor 2, transforming growth factor β, and NOTCH ligands and receptors in adipose stem cells [32,33].

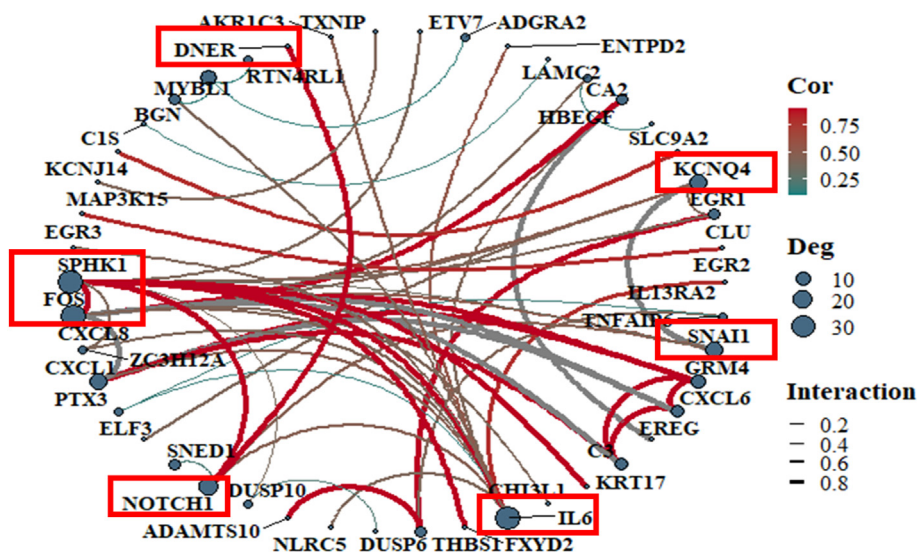


Fig. 7. The constructed PPI networks of the DEGs in EF group and NO EF group. PPI network of the 86 DEGs identified in significant enrichment pathway (adjusted $P < 0.05$) by the KEGG pathway analysis in EF group and NO EF group. Among them, 7 genes were extracted: NOTCH1, SNAIL, IL-6, DNER, FOS, SPHK1, and KCNQ4.

Other genes extracted by PPI network, such as DNER, SPHK1, KCNQ4 and FOS are also involved in angiogenesis regulation. For example, the DNER, Notch1, β -catenin, and ERBB4 appeared to be highly correlated with PSEN1 which promotes vascular remodeling [34]. SphK1, which is a component of FGF1, a widely expressed proangiogenic factor involved in tissue repair and carcinogenesis [35], export pathway.

5. Conclusions and prospects

In summary, these results identified that EF-induced pre-vascularized engineered dental pulp tissue not only had odontoblasts, but also had a rich vascular network, and smooth muscle-like cells appeared around the blood vessels, indicating that EFs significantly promoted the maturation and stable of 3D engineered pulp tissue. In addition, these findings, for the first time, revealed the overall characteristics of EF-regulated vascularization in 3D environment from the perspective of transcriptomic profiles. However, this study has several limitations. First, for the co-culture system with 2 cell types, unlabeled hDPSCs did not distinguish them from endothelial cells. On the one hand, functional cells in the constructed pulp tissue such as smooth muscle cells may not be sure of their origin; on the other hand, the interaction between DPSCs and HUVECs and the alteration of this interaction under electrical stimulation conditions may require further demonstrate in a co-culture system with clear markers distinguishing the two cell types. Second, further studies are needed to determine the effect of electrical stimulation on the differentiation of DPSCs. Third, further study should be conducted *in vivo* to investigate integration of pre-vascularized dental pulp tissue into host tissue. Last but not least, the biological functions of several DEGs, including NOTCH1, SNAIL, and IL-6 in the EF-regulated vascularization in 3D environment remained unclear and should be further explored by *in vitro* and *in vivo* studies.

Ethics approval and consent to participate

Handling of human tissues was done after obtaining the patient's informed consent. According to the ethical principles of The National Health and Family Planning Commission (2016), WMA

Declaration of Helsinki (2013) and CIOMS International Ethical Guidelines for Biomedical Research in Human Body (2002), the studies were approved and monitored by the Hospital of Stomatology of Jilin University Research Ethics Committee (SB (2022) Study No. 48).

Availability of data and materials

All data generated or analyzed during this study are included in this published article.

Funding

The research was supported by “College students Innovation and Entrepreneurship Training Program” of Jilin University (202310183320) and “Medical Science + X” cross-innovation team of the Norman Bethune Health Science of Jilin University (2022JBG510).

Author contributions

Xiaoting Meng and Zhiyong Dong: Conception, design, and supervision. Yingtong Wang and Jiaying Zhou: Performing the experiments, and data/evidence collection, writing the initial draft. Kai Chen and Yushan Liu: Performing the experiments. Xiao Yu: RNA-seq Data analysis.

Declaration of competing interest

The authors declare that they have no competing interests.

References

- [1] Siddiqui Z, Acevedo-Jake AM, Griffith A, Kadincseme N, Dabek K, Hindi D, et al 2022. Cells and material-based strategies for regenerative endodontics. *Bioact Mater* 2022;14, 234–249.
- [2] Saghiri MA, Asatourian A, Sorenson CM, Sheibani N 2015. Role of angiogenesis in endodontics: contributions of stem cells and proangiogenic and anti-angiogenic factors to dental pulp regeneration. *J Endod* 2015;41, 797–803.
- [3] Ben-Shaul S, Landau S, Merdler U, Levenberg S 2019. Mature vessel networks in engineered tissue promote graft-host anastomosis and prevent graft thrombosis. *Proc Natl Acad Sci U S A* 2019;116, 2955–2960.

- [4] Katata C, Sasaki JI, Li A, Abe GL, Nör JE, Hayashi M, et al 2021. Fabrication of vascularized DPSC constructs for efficient pulp regeneration. *J Dent Res* 2021;100, 1351–1358.
- [5] Ruan Q, Tan S, Guo L, Ma D, Wen J 2023. Prevascularization techniques for dental pulp regeneration: potential cell sources, intercellular communication and construction strategies. *Front Bioeng Biotechnol* 2023;111186030.
- [6] Athirasala A, Lins F, Tahayeri A, Hinds M, Smith AJ, Sedgley C, et al 2017. A novel strategy to engineer pre-vascularized full-length dental pulp-like tissue constructs. *Sci Rep* 2017;7, 3323.
- [7] Dissanayaka WL, Hargreaves KM, Jin L, Samaranyake LP, Zhang C 2015. The interplay of dental pulp stem cells and endothelial cells in an injectable peptide hydrogel on angiogenesis and pulp regeneration in vivo. *Tissue Eng* 2015;21, 550–563.
- [8] Cunha F, Rajnecik AM, McCaig CD 2019. Electrical stimulation directs migration, enhances and orients cell division and upregulates the chemokine receptors CXCR4 and CXCR2 in endothelial cells. *J Vasc Res* 2019;56, 39–53.
- [9] Marsano A, Maidhof R, Luo J, Fujikara K, Konofagou EE, Banfi A, et al 2013. The effect of controlled expression of VEGF by transduced myoblasts in a cardiac patch on vascularization in a mouse model of myocardial infarction. *Bio-materials* 2013;34, 393–401.
- [10] Carmeliet P, Jain RK 2011. Molecular mechanisms and clinical applications of angiogenesis. *Nature* 2011;473, 298–307.
- [11] Liu P, Zhang Y, Ma Y, Tan S, Ren B, Liu S, et al 2022. Application of dental pulp stem cells in oral maxillofacial tissue engineering. *Int J Med Sci* 2022;19, 310–320.
- [12] Kim SG 2021. A cell-based approach to dental pulp regeneration using mesenchymal stem cells: a scoping review. *Int J Mol Sci* 2021;22.
- [13] Meng XT, Du YS, Dong ZY, Wang GQ, Dong B, Guan XW, et al 2020. Combination of electrical stimulation and bFGF synergistically promote neuronal differentiation of neural stem cells and neurite extension to construct 3D engineered neural tissue. *J Neural Eng* 2020;17056048.
- [14] Bai H, McCaig CD, Forrester JV, Zhao M 2004. DC electric fields induce distinct preangiogenic responses in microvascular and macrovascular cells. *Arterioscler Thromb Vasc Biol* 2004;24, 1234–1239.
- [15] Xiong GM, Do AT, Wang JK, Yeoh CL, Yeo KS, Choong C 2015. Development of a miniaturized stimulation device for electrical stimulation of cells. *J Biol Eng* 2015;9, 14.
- [16] Chen Y, Ye L, Guan L, Fan P, Liu R, Liu H, et al 2018. Physiological electric field works via the VEGF receptor to stimulate neovessel formation of vascular endothelial cells in a 3D environment. *Biol Open* 2018;7.
- [17] Ramasamy SK, Kusumbe AP, Wang L, Adams RH 2014. Endothelial Notch activity promotes angiogenesis and osteogenesis in bone. *Nature* 2014;507, 376–380.
- [18] Khayat A, Monteiro N, Smith EE, Pagni S, Zhang W, Khademhosseini A, et al 2017. GelMA-encapsulated hDPSCs and HUVECs for dental pulp regeneration. *J Dent Res* 2017;96, 192–199.
- [19] Li Z, Wu M, Liu S, Liu X, Huan Y, Ye Q, et al 2022. Apoptotic vesicles activate autophagy in recipient cells to induce angiogenesis and dental pulp regeneration. *Mol Ther* 2022;30, 3193–3208.
- [20] Quispe-Salcedo A, Ida-Yonemochi H, Nakatomi M, Ohshima H 2012. Expression patterns of nestin and dentin sialoprotein during dentinogenesis in mice. *Biomed Res* 2012;33, 119–132.
- [21] Matsui M, Kobayashi T, Tsutsui TW 2018. CD146 positive human dental pulp stem cells promote regeneration of dentin/pulp-like structures. *Hum Cell* 2018;31, 127–138.
- [22] Shibui T, Hosoya A, Takebe H, Takahashi M, Seki Y, Fujii S, et al 2023. Immunohistochemical localization of CD146 and alpha-smooth muscle actin during dentin formation and regeneration. *Anat Rec* 2023;306, 2199–2207.
- [23] Sui B, Wu D, Xiang L, Fu Y, Kou X, Shi S 2020. Dental pulp stem cells: from discovery to clinical application. *J Endod* 2020;46, S46–S55.
- [24] Yu X, Meng X, Pei Z, Wang G, Liu R, Qi M, et al 2022. Physiological electric field: a potential construction regulator of human brain organoids. *Int J Mol Sci* 2022;23.
- [25] Meng X, Arocena M, Penninger J, Gage FH, Zhao M, Song B 2011. PI3K mediated electrotaxis of embryonic and adult neural progenitor cells in the presence of growth factors. *Exp Neurol* 2011;227, 210–217.
- [26] Luo Z, Shang X, Zhang H, Wang G, Massey PA, Barton SR, et al 2019. Notch signaling in osteogenesis, osteoclastogenesis, and angiogenesis. *Am J Pathol* 2019;189, 1495–1500.
- [27] Fernández-Chacón M, García-González I, Mühleder S, Benedito R 2021. Role of Notch in endothelial biology. *Angiogenesis* 2021;24, 237–250.
- [28] Li ZX, Chen JX, Zheng ZJ, Cai WJ, Yang XB, Huang YY, et al 2022. TGF- β 1 promotes human breast cancer angiogenesis and malignant behavior by regulating endothelial-mesenchymal transition. *Front Oncol* 2022;121051148.
- [29] Rodríguez P, Higuera MA, González-Rajal A, Alfranca A, Fierro-Fernández M, García-Fernández RA, et al 2012. The non-canonical NOTCH ligand DLK1 exhibits a novel vascular role as a strong inhibitor of angiogenesis. *Cardiovasc Res* 2012;93, 232–241.
- [30] Wu ZQ, Rowe RG, Lim KC, Lin Y, Willis A, Tang Y, et al 2014. A Snail1/Notch1 signalling axis controls embryonic vascular development. *Nat Commun* 2014;5, 3998.
- [31] Timmerman LA, Grego-Bessa J, Raya A, Bertrán E, Pérez-Pomares JM, Díez J, et al 2004. Notch promotes epithelial-mesenchymal transition during cardiac development and oncogenic transformation. *Genes Dev* 2004;18, 99–115.
- [32] Zhang Y, Lv P, Li Y, Zhang Y, Cheng C, Hao H, et al 2023. Inflammatory cytokine interleukin-6 (IL-6) promotes the proangiogenic ability of adipose stem cells from obese subjects via the IL-6 signaling pathway. *Curr Stem Cell Res Ther* 2023;18, 93–104.
- [33] Gao W, Sweeney C, Walsh C, Rooney P, McCormick J, Veale DJ, et al 2013. Notch signalling pathways mediate synovial angiogenesis in response to vascular endothelial growth factor and angiopoietin 2. *Ann Rheum Dis* 2013;72, 1080–1088.
- [34] Shen T, Shi J, Zhao X, Fu L, Wang N, Han J, et al 2024. Presenilin 1 is a therapeutic target in pulmonary hypertension and promotes vascular remodeling. *Am J Respir Cell Mol Biol* 2024;70 (6), 468–481.
- [35] Kacer D, McIntire C, Kirov A, Kany E, Roth J, Liaw L, et al 2011. Regulation of non-classical FGF1 release and FGF-dependent cell transformation by CBF1-mediated notch signaling. *J Cell Physiol* 2011;226, 3064–3075.